UA9 report for 2014

Executive Summary

This report describes the UA9 progress of the last 12 months from October 2013. Since no beam was available, the efforts were devoted to complete the prototype crystal collimation system for LHC, to systematically analyze old data, to improve simulation tools and to extend UA9 equipment in the SPS.

Two crystals with their orienting goniometer devices have been installed in the Interaction Region IR7 in **LHC**. The layout has been chosen to reduce significantly the local losses at the limiting locations of the present collimation system, taking into account the optical constraints of the collimation insertion. The goniometer based on a **piezo-electric rotational stage**, designed in collaboration with industrial partners, has been built in two samples and tested. Its performance is suitable for orienting and positioning the crystal with an angular accuracy of 1 μrad as required for the LHC operation. A novel crystal irradiation **test** has been planned in the **HiRadMat** facility at the LHC injection energy. The crystal irradiated in 2012 having been accidentally destroyed, the new test is intended to provide new irradiated crystal to evaluate its deflection efficiency. The design of a **detector** based on **Cherenkov** radiation suited to detect the halo particles deflected by a crystal in the vacuum pipe of the SPS and LHC has been tested at the BTF facility in Frascati. A Cherenkov detector is being produced for installation and test in SPS in 2015. **Multi-strip crystal** for deflecting halo particles by multi-reflection will be tested and compared to single crystals operated in channeling mode. An **extensive data analysis** of the old data collected in H8 has been used for assessing the predictive power of a **MonteCarlo simulation** routine describing particle-crystal interactions. Using the MonteCarlo routine in conjunction with the SIXTRACK accelerator code, a strong background has been observed in the SPS dispersion suppressor, induced by protons deflected by the crystal and not absorbed by the tungsten collimator. This considerably increases the estimated inefficiency of crystal-assisted collimation. A new high-sensitivity beam loss monitor installed in the dispersion suppressor of the SPS should be used in 2015 to confirm our conjecture based on simulation results and on data recorded by standard SPS low-sensitivity beam loss monitors. The possibility of testing crystal assisted extraction in the SPS and of identifying a scenario for **LHC halo extraction** will be considered in the future. This activity will be to a large extent funded by a EU-ERC grant of the INFN.

CERN-SPSC-2014-034 / SPSC-SR-147
15/10/2014

Several **publications** were issued to illustrate the UA9 results. Progress on Cherenkov detectors were presented in various conferences. Test of multi strip silicon deflectors were reported in Nuclear Instruments and Methods in Physics Research B 338 (2014) 108–111. Crystal with focusing effect was discussed in Physics Letters B 733 (2014) 366–372. Mirroring effect of ultra short crystals was shown in Physics Letters B, Volume 734, 27 June 2014, Pages 1-6. Stochastic deflection of positive particles in silicon crystal was presented in Physics Letters B 731(2014)118–121. Progress on data analysis and simulations were discussed in four paper submitted to the PAC 2014 (Particle Accelerator Conference in 2014).

A master and a doctoral **thesis** have been completed in 2014. A PhD and a master thesis are in progress.

Recall of the previous UA9 findings

The results described below are extracted from Ref [1, 2].

The UA9 results, collected in the **SPS with protons and Pb ions at 120 GeV/c and 270 GeV/c per charge**, give a clear evidence of our understanding and our ability to master crystal-assisted collimation.

1. With a **1 mm-long crystal**, fully suited to the SPS stored beam energy, in channeling orientation the loss rate recorded downstream the crystal is reduced by a **factor of about 20** whilst the loss rate in the high dispersion area downstream of the crystal is reduced by **a factor 7**.

2. The beneficial effect of using a crystal primary collimator to deflect the beam halo is global. Although the electronics of the SPS beam loss monitors is not fully adequate for the UA9 running conditions, consistent and reliable indications are available on the fact that the loss map around the entire SPS circumference shows strong reduction of losses in channeling orientation.

3. Crystal-assisted collimation of **ion** beams is **effective** with similar performance as for proton beams

Preparing the test of crystal-assisted collimation in LHC

Following the recommendations of the SPSC referees and the conclusions of the 107th LHCC meeting, the UA9 Collaboration focused most of the activity during LS1 on the

extension to the LHC of the crystal-assisted collimation experiment, with the aim of demonstrating crystal-assisted halo suppression at the LHC. The main goal of the test called **LUA9** is to allow a **direct comparison of the collimation cleaning efficiency with and without the use of crystals**. Operational challenges such as the stability of crystal alignment, the capability of keeping it parallel to the beam envelope during the ramp and the beta-squeezing and the effectiveness of crystal collimation on ion beams will also be addressed.

Additional devices have been installed in Interaction Region 7 (IR7) of the Ring 1 and space has been reserved for future staged installation of other equipments, accordingly to the layout shown in Fig. 1. The two key systems are already in place and are fully operational: each of them is made of a bent crystal supported by a frame and mounted on a moving device that can bring the crystal close to the halo and orient the crystalline planes parallel to the incoming particles. Two crystals will be used to deflect the halo particles in the vertical and in the horizontal directions respectively. Examples of the horizontally and vertically deflected halo particle trajectories with respect to the 6σ circulating beam at top energy are shown in Fig. 2. The deflected particles should be absorbed by secondary collimators already in place, which are part of the standard collimation system, shown in Fig 1. LUA9 will profit of the already existing beam loss instrumentation to observe and optimize the channeling process for halo collimation. To complement the standard instrumentation two novel very fast beam loss monitors made of diamond detectors have been installed downstream of the two deflecting crystals and five more will be added at a later stage, as shown in Fig. 1. Space is also reserved for two CpFM-like detectors (see below) devoted to count the deflected particles.

Cleaning considerations guided the selection of the horizontal and vertical crystal /goniometer positions. Unpublished results of tracking simulations, shown in Fig 3, predict a local cleaning inefficiency 10 times smaller for LUA9 than with the standard collimation system.

Tests of crystal assisted collimation will be performed in LHC, in strict cooperation with the Collimation Team, during dedicated machine development periods at low intensity, at both injection and collision energy in 2015 and/or 2016.

High-precision goniometers and crystals

The goniometers for LUA9 have been designed and produced with the help of industrial partners. The specifications are fully compliant with the requirements of LUA9. A particular

attention was given to provide a linear and accurate rotational movement and to minimize the mechanical play and coupling between the linear and angular movement.

Another crucial requirement was to avoid any possible detrimental effect on the LHC operation with high-intensity beams. Care was taken to mask stray fields in the goniometer itself. Whenever not in operation the crystal and the goniometer should be retracted in a garage position and a sliding vacuum pipe with standard dimension should replace them making them invisible to the beam. This precaution should guarantee to keep unchanged the impedance budget and to avoid the potential onset of coherent instabilities at high circulating intensity. Dedicated measurements have confirmed that in garage position mode, the LHC impedance budget will stay unchanged.

In order to satisfy the specifications on control robustness and reliability within the harsh environmental conditions, the linear axes are actuated by hybrid stepping motors and the positioning is therefore performed in open loop, which represents a more robust control solution. Linear Variable Differential Transformers (LVDT) are chosen to monitor the linear positioning of the axes, to guarantee reliability in harsh conditions and to improve the positioning accuracy and the control robustness. The results of a deep metrological characterization on the installed devices have shown the fulfillment of all the specifications in steady conditions.

To guarantee the angular accuracy required, the piezoelectric actuated goniometer, shown in Fig. 4, has been built with the following functionality:

i. The crystal can be linearly moved perpendicular to the beam with a stroke of 60 mm and a linear resolution of 5 μm.
ii. The crystal can be rotated for a yaw angular range of ±10 mrad with an angular resolution of 0.1 μrad and an angular accuracy of ±1 μrad over the entire linear stroke range.
iii. During rotational movements the overshoot of the yaw angle is of about 2 %, whilst the settling time to within 99% of the final value is of 100 ms.
iv. The device can be safely baked out at a temperature of 110 °C.
v. The device can tolerate a total accumulated radiation dose of 1 MGy.
vi. The goniometer can be installed using the standard LHC Collimator quick-plug support system for a safe and quick intervention in case of fault.
vii. During normal LHC operation the goniometer is fully transparent.

The design incorporates a piezoelectric actuated rotational stage mounted on a high precision linear axis, which together allow the rotational and linear specifications to be satisfied.

The high accuracy of the rotational positioning is achieved using real-time, closed-loop control of the crystal rotational position having an interferometric system as the feedback sensor. The parasitic angles in the planes perpendicular to the operational one are corrected during crystal installation by fine-tuning adjustment stages. The high precision linear stage has a guidance system designed for high repeatability and decoupling of the linear position from the angular position.

The piezoelectric goniometers for horizontal and the vertical planes are identical and have been installed rotated by 90° degrees.

The LUA9 crystals mounted in the two goniometers are made of silicon and have a 4 mm length. The **horizontal crystal**, shown in Fig. 5, is made of a 35 mm high, 4 mm thick strip with 51 μrad bending angle imparted by the anticlastic reaction to the main bending; it will exploit the (110) plane channeling effect. The surface roughness is of about 2 nm. No amorphous layer is present in front of the first crystalline plane. The miscut angle between the surface and the crystalline planes is about 6 μrad. The crystal support is made of grade-V titanium to keep the total weight below 90 g. The residual torsion due to the non-parallelism of the clamping devices is corrected to below 1 μrad/mm. The **vertical crystal** is made of a 4 mm thick plate with 44 μrad quasimosaic bending angle, using the (111) planes to channel particles. An amorphous layer of about 200 nm is present in front of the first crystalline plane. The miscut angle between the surface and the crystalline planes is about 6 μrad. The crystal torsion at the centre is of the order of 1 μ rad/mm with a saddle curvature of 6 μrad/mm. The crystal support is made of grade V titanium to keep the total weight below 90 g.

Crystal irradiation test

Crystal deflectors for crystal-assisted collimation could accidentally be exposed to a not negligible fraction of the nominal beam intensity. In these extreme conditions, a reliable knowledge of thermal and radiation effects is required, to prevent the potential degradation of the channeling efficiency and, in the worst case, the mechanical stability. In particular, one concern to be addressed is the crystal integrity in case of an accidental scenario such as an asynchronous beam dump or a badly steered injection of a particle batch where bunches could be deflected onto the crystal. A first indication of possible effects on crystal deflectors can be inferred from previous irradiation tests with high-energy proton beams performed at different facilities [4, 5], where no macroscopic damage but some degradation of the channeling

efficiency was observed for an irradiation density of 2.4×10^{20} protons/cm^2 at 440 GeV. However, to realistically probe the mechanical strength of a crystal under beam impact conditions imposed by the LHC operational environment, dedicated irradiation tests have been carried out at the CERN HiRadMat facility. The test in Ref [6] was performed with a 440GeV proton beam irradiating a 3 mm-thick silicon strip crystal produced at INFN-Ferrara, with properties comparable to those of the LHC deflecting crystals. The tests were carried out with the crystal in amorphous orientation. The crystal was aligned to the incoming beam position and high-intensity pulses were extracted from the SPS. The normalized transverse emittance as measured with the SPS beam wire scanner before the high-intensity extractions was approximately 3.5 μmrad in both planes, confirming the desired beam size at 1σ of 0.5×0.5 mm^2 at the position of the crystal. Starting initially with a single bunch, the number of bunches per pulse was gradually increased to 72, 144 and 288 with an average bunch intensity of 1.1×10^{11}. The integrated number of protons extracted during all high-intensity shots was approximately 2×10^{14}. First visual inspections indicated no macroscopic damage to the crystal. Further post-irradiation studies of crystal properties were foreseen in H8 beam line of the SPS North Area. Unfortunately these measurements are no longer possible since the crystal was mechanically broken during a false manipulation of it. The irradiation test will be repeated in 2015.

In-vacuum Cherenkov detector

In its early tests UA9 was able to produce images of the channeling deflected beam during SPS dedicated coast fill. Nevertheless the number of deflected particle was never determined with few percent precision. UA9 started an R&D program with the aim of building a proton flux monitor based on fused silica radiators to be hosted directly into the beam pipe vacuum (named **CpFM**). Channeled protons produce Cherenkov light that is guided by the radiator itself outside the vacuum and detected with a PMT in air. A dedicated electronics is used to record the signal preserving the very good timing information of the light. This would also allow using the CpFM in coincidence with other devices in the UA9 experiment. The device is explicitly designed to meet the SPS and LHC requirements: fused silica is highly radiation resistant and no other material is used in vacuum and in the vicinity of the pipe (like glues or plastic materials). Cherenkov light is routed to the PMT far (few meters) from the beam pipe by fused silica optical fibers to avoid PMT being swamped by radiation background from the accelerator.

In 2014, a prototype Cherenkov radiator has been tested in the BTF facility of the Laboratory Nazionali di Frascati with the aim of selecting the optimal shape. The setup is shown in Fig. 7. Two rectangular bars of hard fused silica (quartz) are used as Cherenkov radiators. One bar is used to measure signal from the incoming beam and another to monitor the background. Due to the total internal reflection, the Cherenkov light is kept inside of the fused silica radiator and propagates towards PMT via fibers bundle. The number of outgoing photons injected into the fibers bundle is maximum when the radiator bar is tilted at 47° with respect to the incoming particles, which is equal to the Cherenkov angle (for ultra-relativistic particle) in fused silica. A movable bellow permits the insertion and extraction of the bars into the deflected beam. A flange inclined by 47° angle with respect to the beam pipe supports the radiators. A radiation hard fused silica viewport with 3 mm thick window is mounted into the flange. It provides optical contact between radiators placed in vacuum and the bundle of fibers placed in air. Two radiation hard bundles composed of fused silica/fused silica (core/cladding) fibers bring the Cherenkov light from radiators to photo-multipliers (PMT). Two R7378A radiation resistant HAMAMATSU PMTs allow detecting the Cherenkov photons. A 10 m long glass fiber and two 300 m long low attenuation CKB50 cables allow simulating the signal attenuation for the installation of the CpFM on either SPS or LHC. The USB-Wavecatcher module [7] for data acquisition is situated 300 m away from the radiators.

The BTF is a beam line designed for detector calibration purposes with single or multiple electrons. The flux of outgoing electrons can be monitored with a lead glass calorimeter capable to separate single incoming electron. We adjusted the beam to get in average 200 electrons of about 500 MeV energy and performed resolution measurements of the Cherenkov assembly. Figure 8 shows the number of photo-electrons (p.e.) detected as a function of the measured charge by the calorimeter. The correlation due to statistic variation of the incoming electrons is observed. Using a linear fit of this dependency, one can perform correction on incoming numbers of electrons and measure the resolution (see Figure 9), which gives 15 % for 100 electrons. The fit with the Gaussian function of this histogram gives 0.62 p.e. per incoming electron. To estimate effect of the viewport between the vacuum inside the beam pipe and atmosphere we performed tests with and without the glass plate of 3.8 mm thickness simulating the viewport itself. The signal intensity at the PTM was reduced by a factor 2 in comparison with a direct coupling. The potential losses of photons due to the contact of an holder with the quartz surface was simulated by putting around the bar different kind of rings made of copper or black tape with width of 0.5 to 1 cm. No degradation of the output signal was observed.

A substantial effort should be made to realize a device that is totally compatible with the LHC requirements for vacuum compatibility, impedance minimization and radiation resistance in the LHC collimation sectors. For instance to avoid any additional mechanical support an R&D (that is still going on) to braze the quartz radiator directly to steel has been carried out. A CpFM device is being produced by an industrial partner and should be installed in the SPS for a test in 2015.

Analysis of the entire data-set collected in H8

An analysis of all the data collected in the H8 line of the SPS North area for a long list of crystals was eventually made. This was done in the view of evaluating the details in crystal-particle interactions and of making reference data available for testing simulation routines.

The detector used in H8 is schematically shown in Fig 9. It contains a two-axis goniometer that can houses crystals in their bending holders. Five detector planes made of silicon strips allow measuring the particle trajectories with an angular accuracy of 5.5 μrad. Generally, the data taking consists in recording the angular deflection of a particle as a function of the crystal angle with respect to the direction of the incoming particles.

Two subtle effects never observed before have been singled out. The first consists in the increase of the dechanneling probability for channeled particle with large transverse energy. Particles oscillating between two crystalline planes have a larger probability of a nuclear interaction for larger oscillation amplitudes. The other effect consists in an exponential variation of the volume capture probability as the crystal angle increases with respect to the channeling angle. These two observations are yet unpublished.

The other point is the identification of a high statistics set of data collected in channeling mode and its exploitation to determine with high precision important parameters such as the probabilities of channeling, volume reflection and dechanneling. Comparing these data with simulation results allowed us evaluation how predictive the simulation can be. In Fig. 11 we show the very high-statistics set of data relative to the strip crystal STF45. In Fig 12 we show how these data can be used to estimate the probabilities of the various crystal-particle process. In Fig. 13 we present a comparison with the single-pass code used to simulate crystal-particle interactions using a MonteCarlo method. When taking into account the detector accuracy the agreement between simulation and experimental data is very good, i.e. better than 10%. The same data have also been used to check results of other simulation routines based on the integration of the equation of motion of a charged particle in a crystal and on the statistic

evaluation of the probability of nuclear reactions or scattering with electrons. Also in this case the results are in a rather good agreement. The above mentioned simulation routines are used also in general simulation codes to describe the behavior of crystal in circular accelerators. The MonteCarlo based routine is particularly fast and perfectly suited to be inserted in the SIXTRACK code, also used for evaluation of the LHC collimation system. The routines based on step-by-step integration will be used in FLUKA and GEANT4. The scrutiny of the simulation routine used in SIXTRACK is particularly important for what discussed in the following Section.

Simulation of the SPS data

The simulation code SIXTRACK, describing beam dynamics in circular accelerators, specifically used to investigate features of the LHC collimation systems, was recently extended to include the last version of MonteCarlo based routine describing crystal-particle interactions. This provided us a new tool to perform realistic simulations of the old UA9 experimental results in the SPS.

The main outcome of the new simulation campaign was the strong indication of an unexpectedly large off-momentum background in the dispersion suppressor area, resulting in the **overestimation** of the **crystal-assisted collimation inefficiency**. The collimation inefficiency of the two-stage crystal collimation system in the SPS is deduced from the beam-loss rate registered in the high-dispersion area with the crystal in channeling mode and in amorphous orientation. In the tests of last years, the measured loss rate is reduced by a factor 7 when changing the crystal orientation from amorphous to channeling mode [2,3]. The recent simulation results have shown that losses in the high-dispersion location downstream of the crystal have two sources. One is the diffractive events in the crystal that produce off-momentum protons reaching the vacuum pipe in the dispersive area down-stream of the crystal itself. The other are the deflected protons that cross the 60 cm long tungsten absorber (called TAL) and reach the dispersive area too, since their trajectories stay in the accelerator acceptance at the exit of the TAL. This situation is schematically shown in Fig. 14, where the SPS lattice is plotted with the dispersive function in the region of the crystal collimation devices and in the dispersion suppressor downstream. Main dipoles and quadrupoles are shown in red and blue respectively. The locations of the crystal of the TAL and of the BLMs are also indicated. Table 1 gives the loss probability computed with SIXTRACK. It is clearly visible that the expected value of the losses at the BLM5 is strongly influenced by the background induced by the halo protons not absorbed by the TAL. Those particles emerge

with a reduced momentum because of the ionization interactions with tungsten absorber. They then reach the location close to the BLM7 and the simulations also indicate that at the position of the BLM7 the contribution of those particles to the losses should be large. In fact, the loss rate recorded by the standard low-sensitivity SPS beam loss monitor in that position give a reduction factor of 20 in a good agreement with the simulation results. A high-sensitivity BLM has been installed in the position of the BLM7 and a new measurement in 2014/15 will be performed to clarify this very important issue. Note that in LHC no background is expected to survive after the secondary absorber traversal.

Table 1: Loss probability in the SPS crystal collimation simulation.

Location	Crystal orientation	Losses from crystal	Losses from TAL	Total losses	Losses reduction
BLM5	AM	$4.7\ 10^{-5}$	$1.2\ 10^{-3}$	$1.2\ 10^{-3}$	
BLM5	CH	$7.7\ 10^{-7}$	$1.7\ 10^{-4}$	$1.7\ 10^{-4}$	~7
BLM7	AM	$1.5\ 10^{-4}$	$4.2\ 10^{-5}$	$4.3\ 10^{-5}$	
BLM7	CH	$2.1\ 10^{-6}$	$6.9\ 10^{-6}$	$9.0\ 10^{-6}$	~21

Extraction assisted by bent crystals

Crystals with large bending angle (~1 mrad) could be used for the extraction of a portion of a circulating beam. This has been successfully demonstrated at CERN SPS by the RD22 experiment and routinely used at the U70 Protvino proton accelerator. Current technology advance in crystal manufacturing that UA9 collaboration has contributed to in the last years would allow a scheme for a parasitic extraction of the LHC beam even at the 7 TeV energy.

INFN has recently obtained a EU funded ERC grant (named ***CRYSBEAM***) to study such an extraction scheme based on crystals oriented with a high precision goniometer in vacuum. This project includes also the development of a Cherenkov-light based detector (an advanced version of the UA9 CpFM) for a better monitoring of the beam. Moreover, the project aims to demonstrate that a measurement of a cross-section in the absorber material is possible by instrumenting the absorber itself. Study of the hadronic shower generated in the absorber would represent an interesting benchmark of comparison for the Monte Carlo code developed to describe the Ultra high energy Cosmic ray interacting in the Earth's atmosphere.

The INFN has officially proposed to include within the UA9 collaboration activity the CRYSBEAM goal. Special crystal will be produced by INFN and hopefully be ready to be tested in the 2015 at the H8 lines. In the meanwhile an advanced version of the Cherenkov detector will be developed to possibly include some position and timing information. A study and simulation of the "smart" absorber will be carried out to define its characteristics.

An extraction scheme will then be proposed and possibly implemented in the UA9 LSS5 region where some space can be made available. This would demonstrate that high efficiency extraction is possible. Hadronic shower measurement would be also carried out in this context.

This would lead in a five year time-span to propose an extraction scheme for LHC itself.

Perspective and Plans

The perspective of the Collaboration includes some ambitious milestones.

In the SPS, the goal is to test the reduction factor of the collimation background with novel beam loss monitor installed in the dispersion suppressor, in view of assessing the right value of the inefficiency of the off-momentum cleaning. Other goals consist in installing a multi-strip crystal to compare its behavior to that of a single strip crystal and in installing and testing Cherenkov radiator in view of a possible usage in LHC. A piezo-electric goniometer, similar to the LHC ones, is being produced and should be installed at the end of 2014. Its test with the SPS beam to be planned in the first half of 2015 is considered essential to gain experience for the LHC test expected in the second half of 2015.

In the H8 area, the plan is to test twin crystals as those installed in the LHC. Another goal is to test multistrip crystal with an optimal mutual orientation of the strips for a further test of multi-reflection in the SPS. Studies of possibility to increase the channeling efficiency using the crystals with decreasing curvature and the crystals with focusing slot will be pursued. Study of crystals with large curvature, suited for crystal-assisted extraction will be initiated.

In LHC, the priority is to start crystal assisted collimation tests in the horizontal and vertical planes.

In view of these plans, the Collaboration would like to request in 2015 20 days in H8 with proton microbeams at 450 GeV and 7 days with ion (Ar or Pb) beams. Five dedicated days (24 h runs in storage mode) in the SPS should allow us testing the dispersion suppressor background reduction factor and the performance of multi-strip. A short single strip crystal, better adapted to the SPS working energy of 270 GeV should provide us more information of the collimation performance in optimal conditions. The test of the high accuracy goniometer will be highly instructive for the LHC test.

References

[1] UA9 status report for 2012.

[2] W. Scandale et al., Phys.Lett. B 714 (2012) 231.

[3] W. Scandale et al. Optimization of the crystal assisted collimation of the SPS beam. Phys. Lett. B 726 (2013) 182.

[4] C. Biino et al., Proceedings of EPAC96, Sitges, Barcelona, Spain, 1996, p. 2385.

[5] V.M. Biryukov et al., Nucl. Inst. Meth. B 234, 2005, p. 23.

[6] A. Lechner et al, Proceedings of IPAC 2013, Shanghai, China, 2013, p. 3427.

[7] D. Breton, et al., Topical Workshop on Electronics for Particle Physics (2009), http://hal.in2p3.fr/in2p3-00421366/en/.

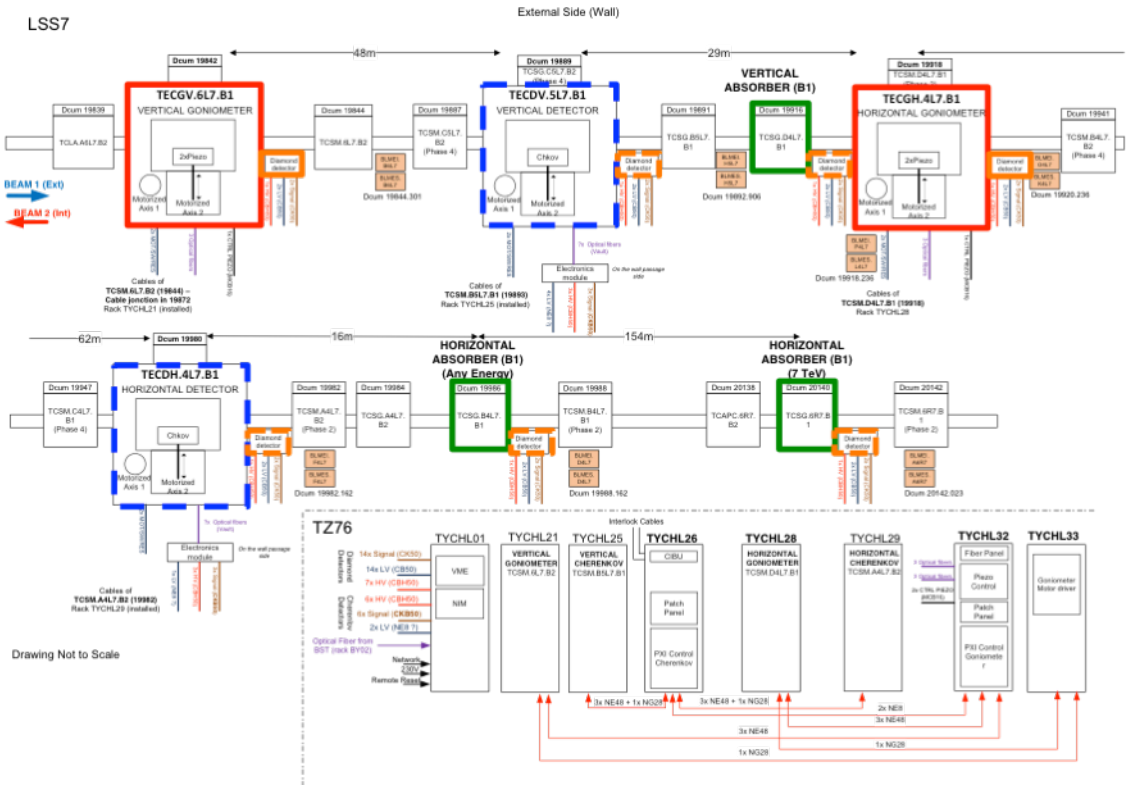

Figure 1 : Layout of the LHC with the crystal-assisted collimation devices inserted or to be inserted in Ring 1. The vertical and the horizontal goniometers are circled in red. The diamond detectors of beam loss are circled in orange. The absorbers of the deflected halo are circled in green. The Cherenkov detectors for the deflected particles are circled in blue. Solid colored lines indicate devices installed. The dashed colored lines indicate spaces which are currently reserved for future installations.

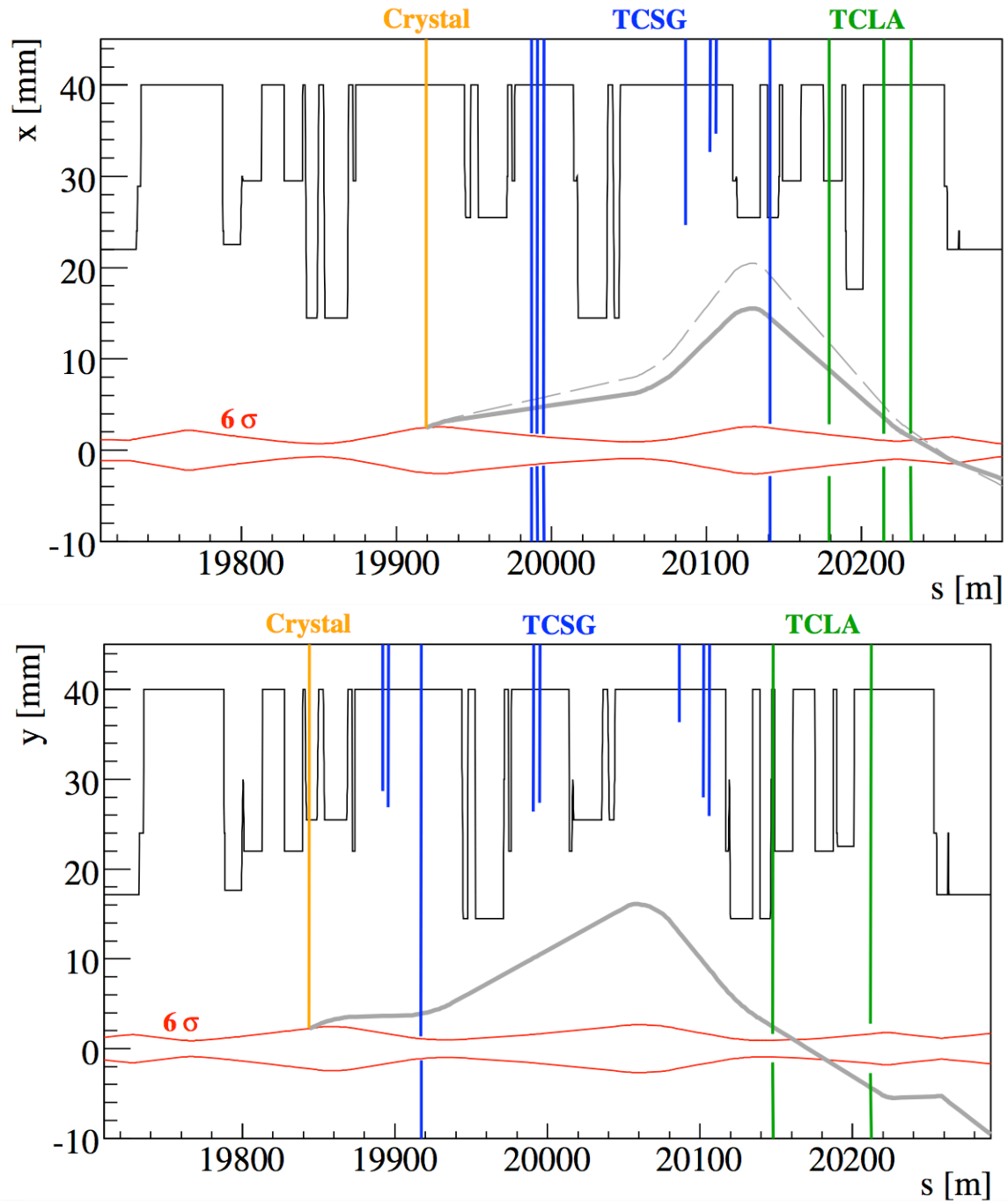

Figure 2 : Trajectories (grey) of the crystal (orange) deflected halo computed at 7 TeV, with respect to the 6σ beam envelope (red). TOP: horizontal trajectory. BOTTOM : vertical trajectory. The location along the LHC Ring 1 of the secondary collimation absorbers is indicated in blue and in green.

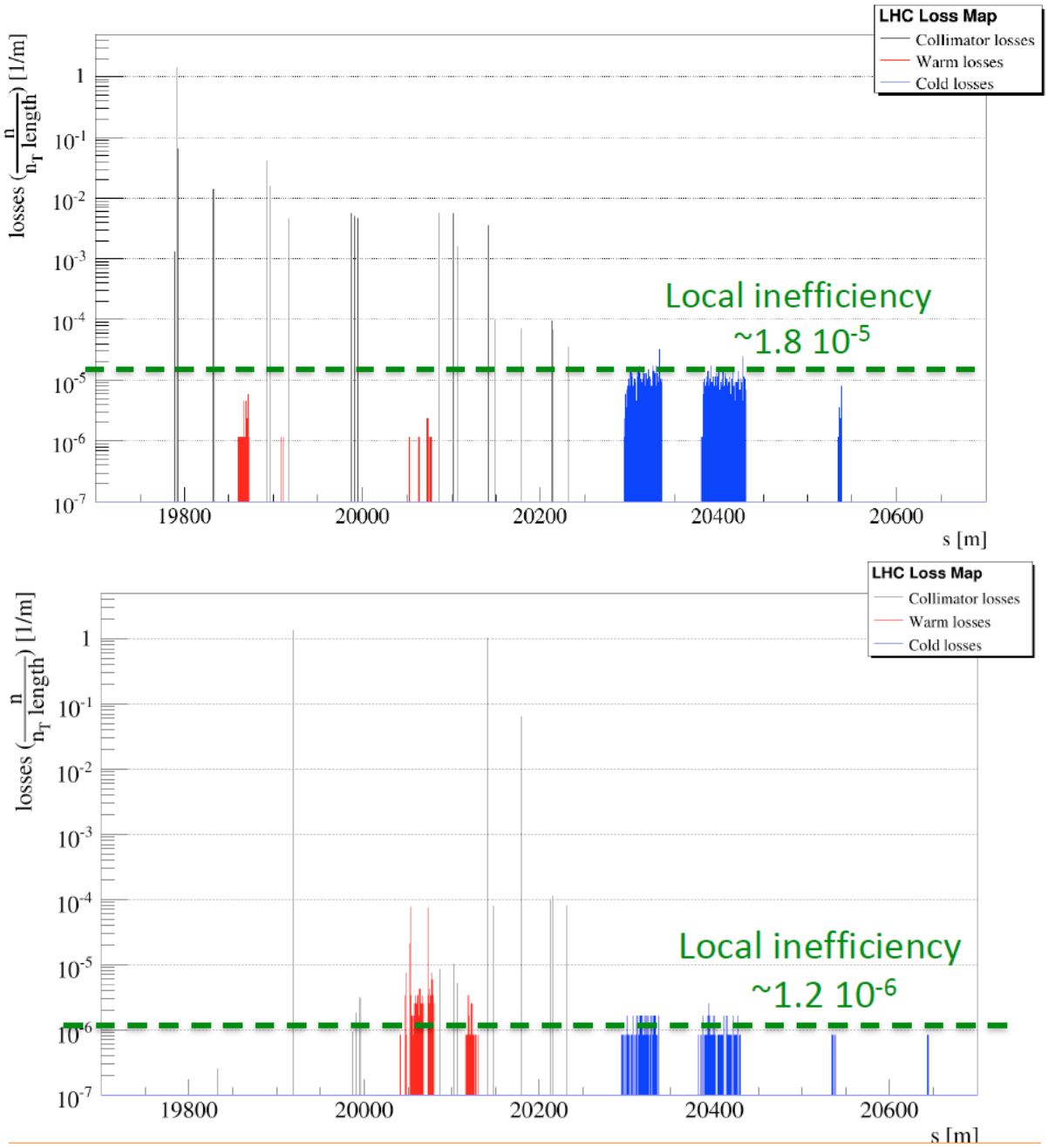

Figure 3 : Loss maps along the collimation sector in IR7 and the subsequent arc in LHC computed at top energy. TOP: standard collimation system. BOTTOM: LUA9 crystal-assisted collimation system.

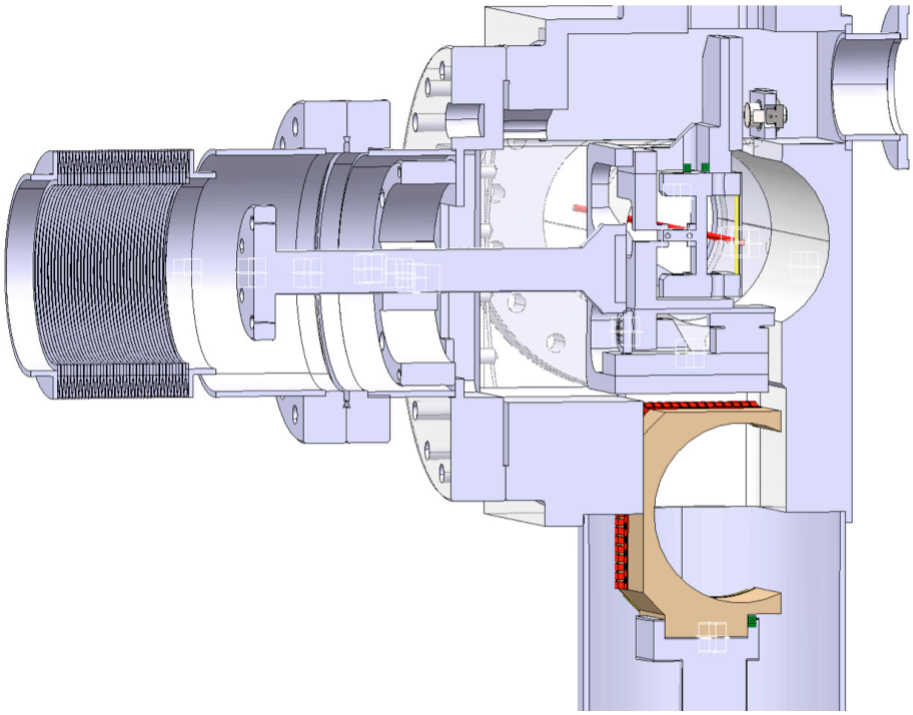

Figure 4 Scheme of the LUA9 goniometer. The crystal is shown in yellow at its operation position. The pipe seen replacing the goniometer in the garage position is shown in brown.

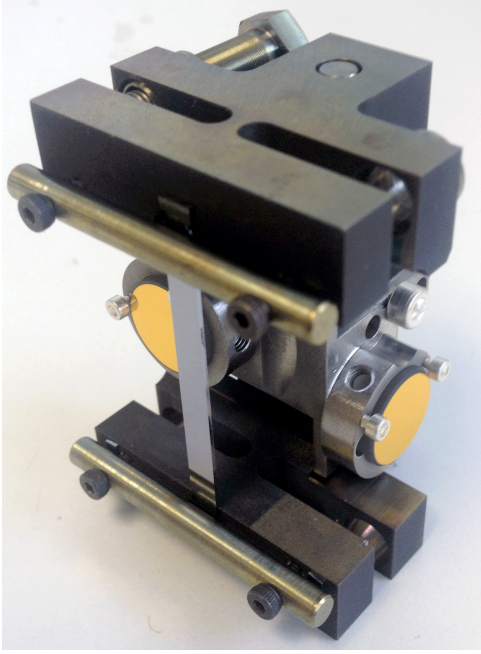

Figure 5 : Strip mono-crystal in its bending support, produced by the INFN- Ferrara. The yellow spots are the gold reflecting plates orthogonal to each other for alignment.

Figure 6 : quasi-mosaic crystal in its bending support, produced by PNPI, Gatchina. The silver spots are the polished regions of the support orthogonal to each other for alignment.

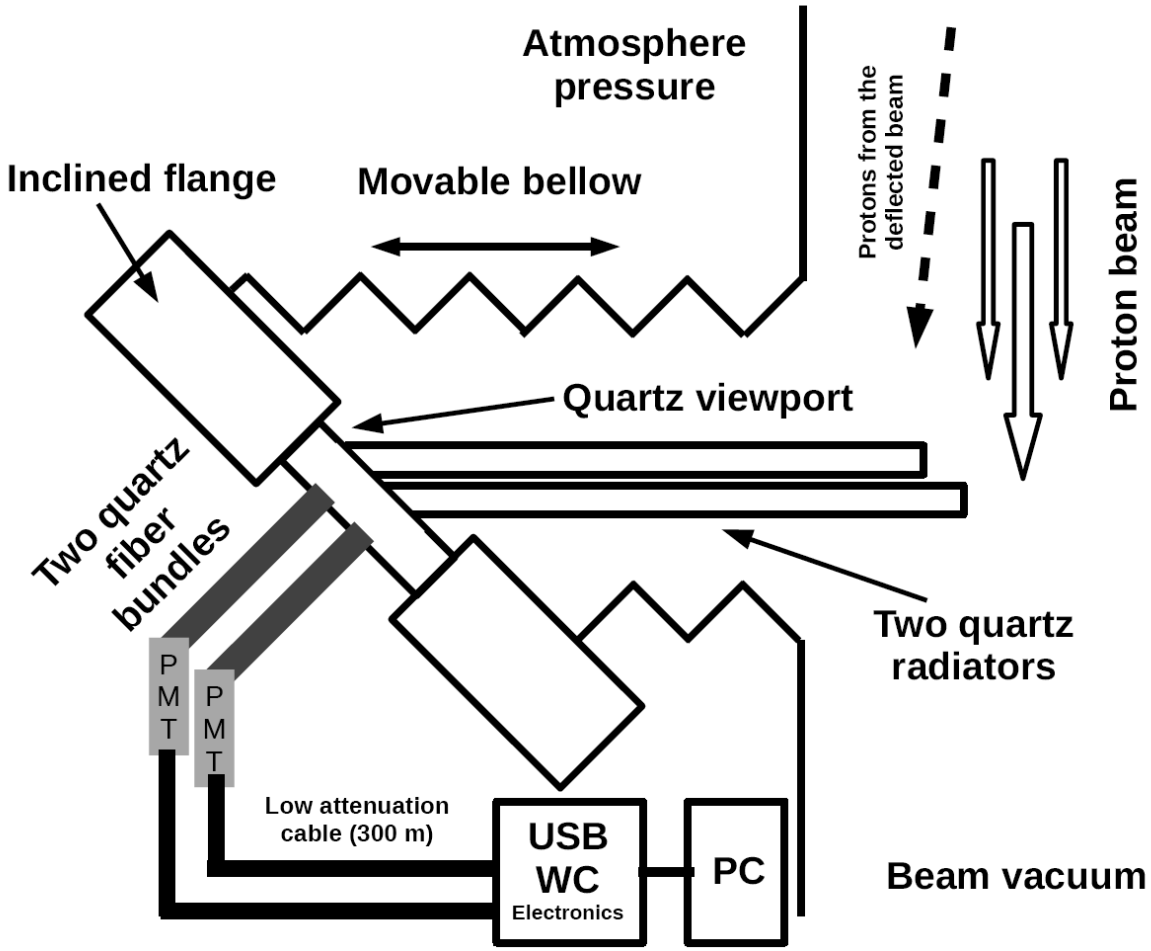

Figure 7 : Scheme of the Cherenkov detector prototype tested at the BTF.

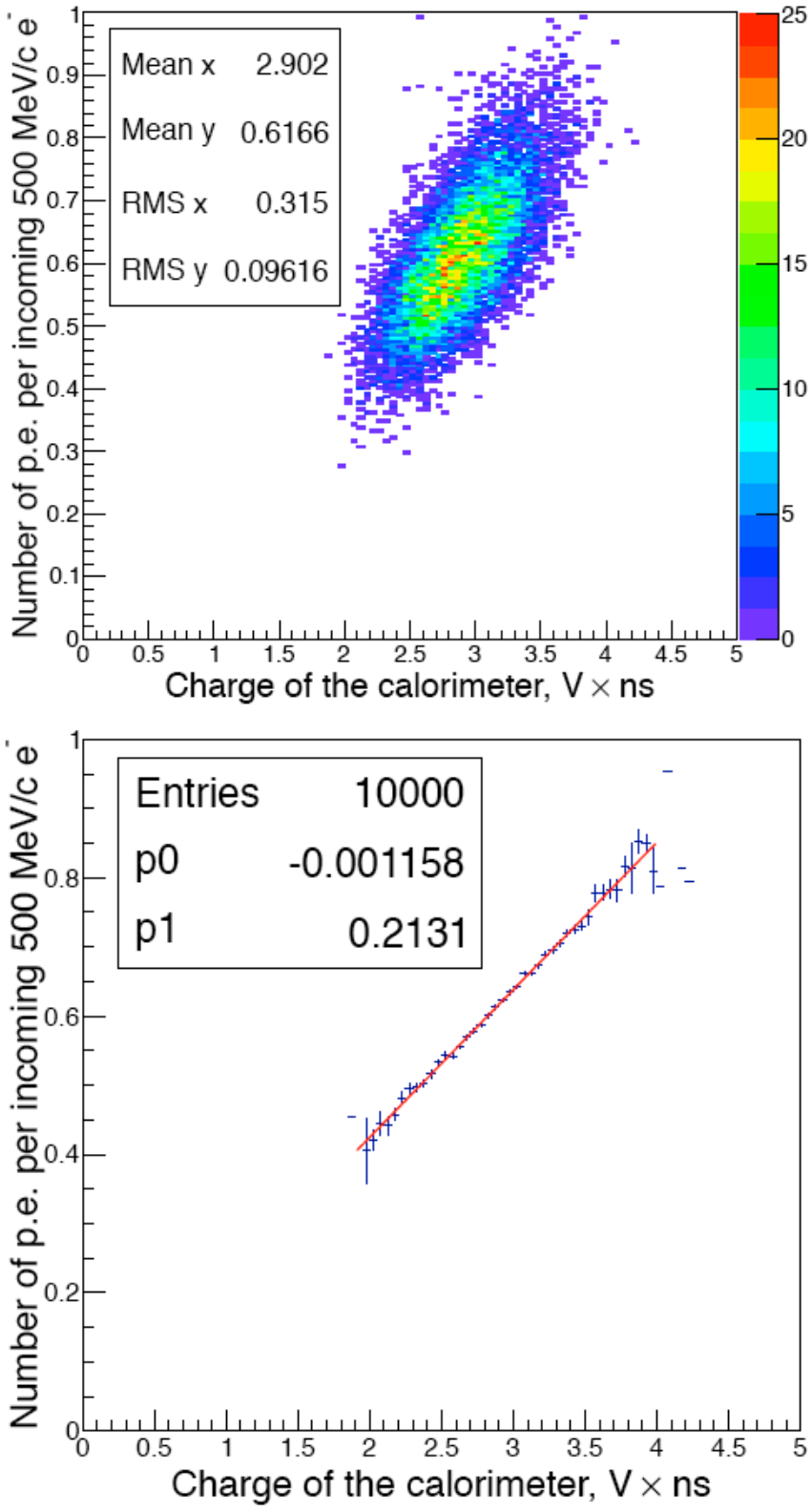

Figure 8 : TOP: 2-dimensional histogram of the number of detected p.e. per incoming 500 MeV electron versus charge measured by the calorimeter. BOTTOM: average number of p.e. versus charge interpolated with a first order polynomial function.

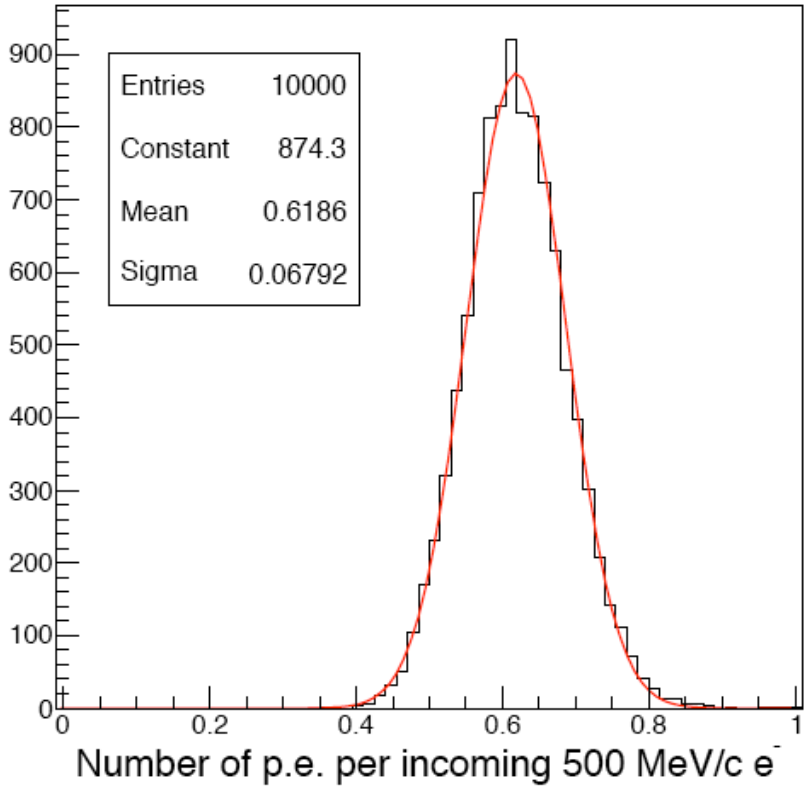

Figure 9 : Number of p.e. measured by the Cherenkov normalized to the number of incoming electrons.

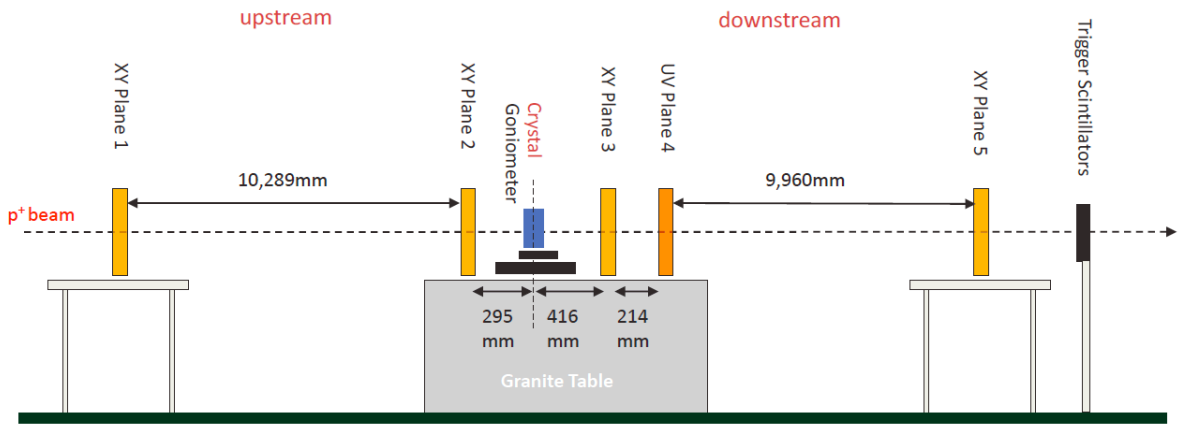

Figure 10 : Devices for the crystal-particle interaction investigations in H8.

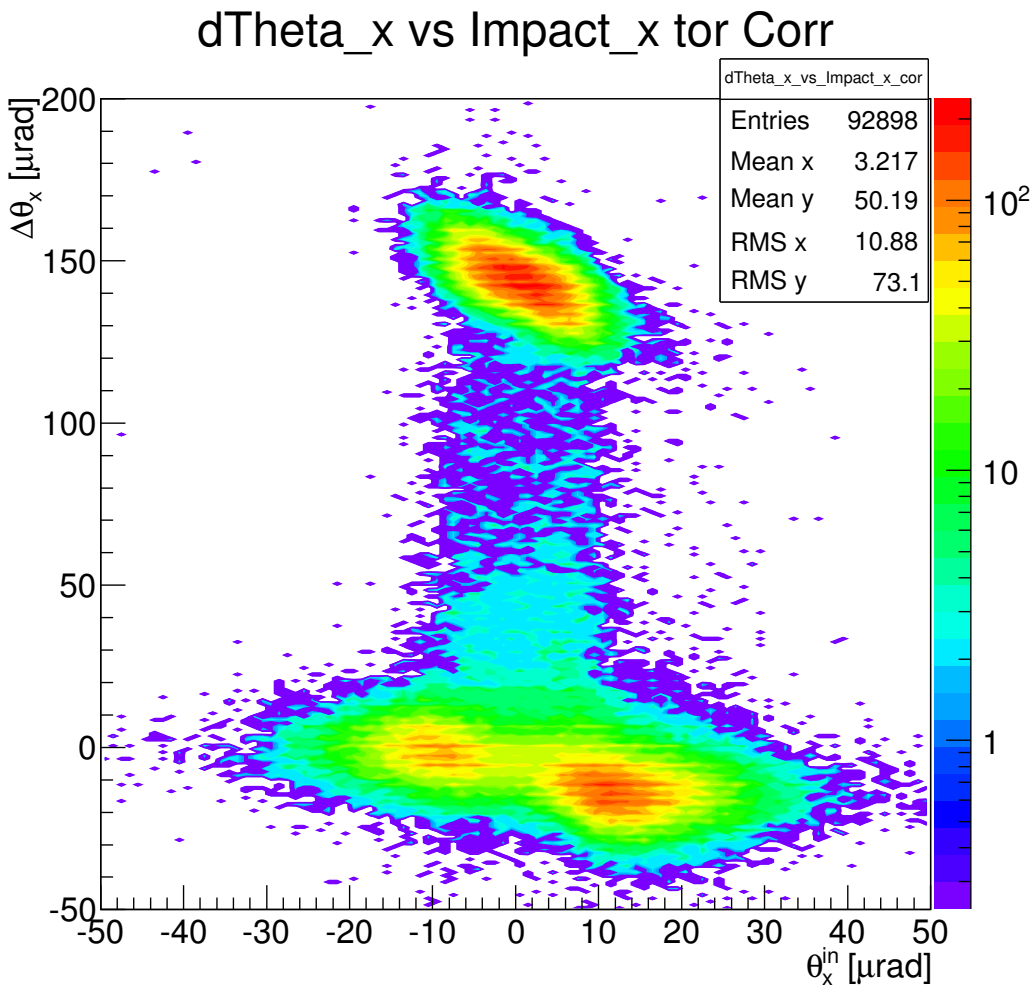

Figure 11 : Particle deflection at a fixed angular position for the crystal STF45.

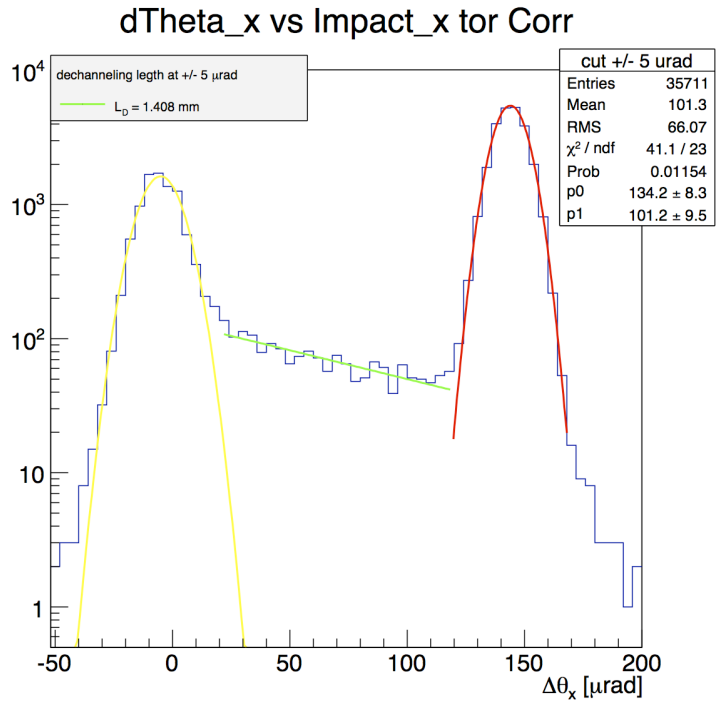

Figure 12 : Projection of the data in Fig. 11, when using a sliding binning of 5 µrad. The red and the yellow Gaussians allow interpolating the channeled and the volume reflected particles, respectively. The green line is used to interpolate the dechanneling process and to evaluate the dechanneling length.

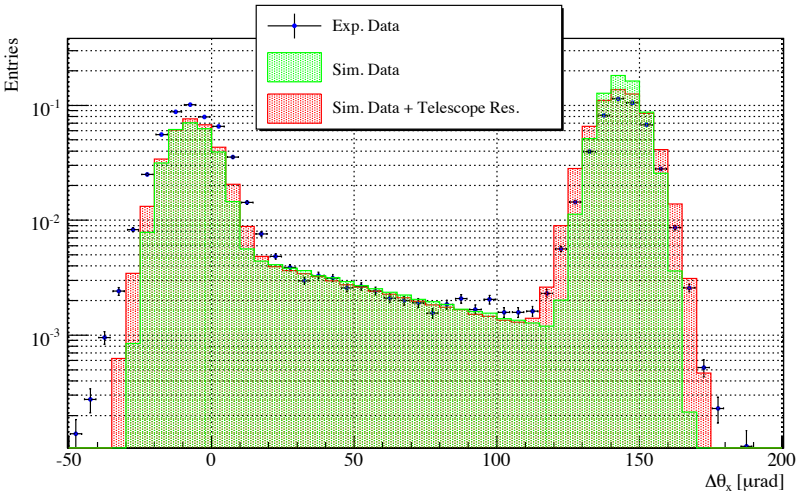

Figure 13 : Projection of the data in Fig. 11 and of simulated events, when using a sliding binning of 5 µrad. The red and the green give interpolations of the simulation events with and without the H8 tracker uncertainty, respectively. The blue cross are the experimental points.

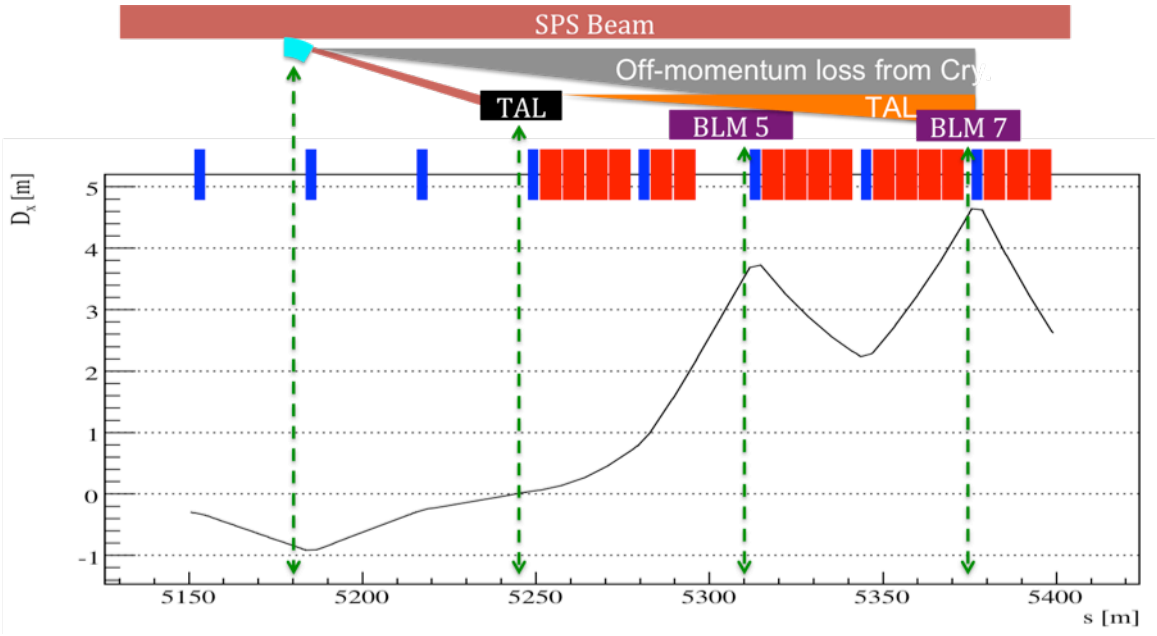

Figure 14 : Off-momentum loss of halo particles in the SPS dispersion suppressor. The losses are partly due to the deflected particles non-absorbed by the tungsten collimator TAL and partly to the diffractive events in the crystal. Dispersion values D_x are shown for the SPS UA9 area. The dispersion suppressor area includes the first two cells with dipoles (from the TAL to the BLM7).